Solution Structure of the Cytoplasmic Domain of Phospholamban: Phosphorylation Leads to a Local Perturbation in Secondary Structure‡

Russell J. Mortishire-Smith,§ Steven M. Pitzenberger,|| Carl J. Burke,⊥ C. Russell Middaugh,⊥ Victor M. Garsky,|| and Robert G. Johnson*,#

Neuroscience Research Centre, Merck Sharp and Dohme Research Laboratories, Terlings Park, Eastwick Road, Harlow, Essex CM20 2QR, United Kingdom, and Departments of Pharmaceutical Research, Medicinal Chemistry, and Pharmacology, Merck Research Laboratories, WP44-L206, P.O. Box 4, West Point, Pennsylvania 19486

Received February 9, 1995; Revised Manuscript Received April 14, 1995⊗

ABSTRACT: Peptides representing the N-terminal domain (Ia) of the cardiac sarcoplasmic reticulum protein phospholamban (residues 1−25 [PLB(1−25)] and a phosphorylated form [pPLB(1−25)]) were synthesized and their conformations examined using circular dichroism and nuclear magnetic resonance spectroscopy. In aqueous solution, both PLB(1−25) and pPLB(1−25) adopt a primarily disordered conformation. In 30% trifluoroethanol/10 mM phosphate, PLB(1−25) exhibits a CD spectrum consistent with 60% helical structure. This value decreases to 27% for the phosphorylated peptide. CD spectra in 2% SDS indicate 40% α-helix for PLB(1−25) and 20% for pPLB(1−25). Full chemical shift assignments were obtained by conventional homonuclear NMR methodologies for both PLB(1−25) and pPLB(1−25) in 30% trifluoroethanol/water and 300 mM SDS. The solution structure of PLB(1−25) in 30% TFE/water was determined from distance geometry calculations using 54 NOE distance constraints and 17 torsion angle constraints. In the family of 20 calculated conformers, the root mean square deviation from the mean structure is 0.79 Å for backbone heavy atoms of residues 1−17. The structure comprises a regular α-helix extending from M1 to S16 with the remaining C-terminal residues disordered. The calculated structure is supported by analysis of $C^{\alpha}H$ secondary shifts which are significantly negative for residues 1−16. Chemical shift degeneracy is substantially more extensive in the phospho form and precludes a direct comparison of calculated structures. However, the magnitudes of upfield secondary shifts are decreased by 20% in residues 1−11 and are not significantly helical for residues 12−16 according to the criteria of Wishart et al. [(1992) *Biochemistry 31*, 1647−1651]. $^3J_{HN\alpha}$ coupling constants measured for I12, R13, A15, and S16 also suggest that residues 12−16 undergo a local unwinding of the helix upon phosphorylation. Similar results are obtained for PLB(1−25) and pPLB(1−25) in 300 mM perdeuterated sodium dodecyl sulfate except that differences in backbone dynamics for the helical and nonhelical regions of the peptide are evident in the DQF-COSY line shapes for fingerprint cross-peaks. This disruption of structure at the C-terminus of the helix suggests a model for phosphorylation-induced dissociation of the PLB/Ca^{2+}-ATPase complex.

Phospholamban (PLB)[1] is a 52-residue protein localized almost exclusively to the cardiac myocyte where it is found subcellularly within the sarcoplasmic reticulum (Tada & Katz, 1982). It binds to the calcium ATPase as an endogenous inhibitor, thereby attenuating the Ca^{2+}-ATPase pump rate (Hicks et al., 1979; Inui et al., 1986; James et al., 1990). Phosphorylation of PLB relieves this inhibition, presumably due to decreased interactions between PLB and the Ca^{2+}-ATPase. *In vivo* and *in vitro* studies have shown that PLB can be phosphorylated at S-16 by protein kinase A or T-17 by calcium−calmodulin-dependent protein kinase (Tada et al., 1974; Kranias, 1985; Movsesian et al., 1984). PLB phosphorylation at either site results in an apparent increase in affinity of the SR Ca^{2+} pump for calcium. It is this effect which is the primary response to β-stimulation of the heart: (a) the positive inotropy is the result of increased calcium accumulation into the SR (and therefore increased release of calcium available to the myofilaments), and (b) the positive lusitropy (increased rate and extent of relaxation) is due to the faster rate of calcium uptake. Recent transgenic mouse phospholamban knockout experiments confirm the critical role of PLB in mediating cardiac contractility (Luo et al., 1994). Unfortunately, the precise nature of the PLB/Ca^{2+}-ATPase interaction is unknown, as is the structure of PLB itself.

‡ Coordinates have been deposited in the Brookhaven Protein Data Bank (file name 1PLP).

* To whom correspondence should be addressed.
§ Merck Sharp and Dohme Research Laboratories.
|| Department of Medicinal Chemistry, Merck Research Laboratories.
⊥ Department of Pharmaceutical Research, Merck Research Laboratories.
Department of Pharmacology, Merck Research Laboratories.

⊗ Abstract published in *Advance ACS Abstracts,* June 1, 1995.

[1] Abbreviations: Ca^{2+}-ATPase, calcium translocating adenosinetriphosphatase; CD, circular dichroism; DPC, dodecylphosphocholine; DQF-COSY, double-quantum-filtered correlation spectroscopy; FAB, fast atom bombardment; HPLC, high-performance liquid chromatography; MOPS, 3-(*N*-morpholino)propanesulfonic acid; NMR, nuclear magnetic resonance; NOE, nuclear Overhauser effect; NOESY, two-dimensional NOE spectroscopy; PLB, phospholamban; PLB(1−25), N-terminal portion of PLB; pPLB(1−25), serine-16 phosphorylated PLB(1−25); SDS, sodium dodecyl sulfate; SR, sarcoplasmic reticulum; TFE, trifluoroethanol; TOCSY, total correlation spectroscopy.

0006-2960/95/0434-7603$09.00/0

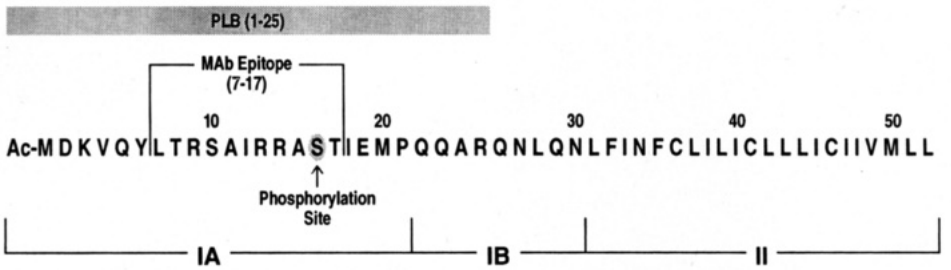

FIGURE 1: Primary sequence of phospholamban emphasizing structural features.

A series of experiments indicate that all (or at least the major) binding site(s) on PLB for the ATPase reside in the N-terminal domain. Trypsinization of cardiac SR produces cleavage of the N-terminal 24 amino acids of PLB and destroys its inhibitory effect (Kirchberger et al., 1986). PLB(1−25), but not PLB(13−35) inhibits Ca^{2+} transport by the Ca^{2+}-ATPase (Hughes et al., 1994). A monoclonal antibody which recognizes an epitope in the region 7−17 of PLB induces dissociation of PLB from the ATPase (Suzuki & Wang, 1986; Kimura et al., 1991; Sham et al., 1991; Briggs et al., 1992). The phosphorylation site of PLB resides in this region (Tada et al., 1974; Kranias, 1985; Movsesian et al., 1984). A number of groups have suggested models for the structure of PLB *in vivo* (Tada & Kadoma, 1989; Young et al., 1989; Toyofuku et al., 1994) (Figure 1). The N-terminal 30 residues comprise a cytoplasmic hydrophilic domain (Ia) which contains both phosphorylation sites. Secondary structure predictions from hydropathy profiles and sequence analysis indicate that domain Ia is likely to be helical. Circular dichroism spectra of intact PLB and peptides encompassing this domain are also consistent with this hypothesis. The precise extent of helix formation within the cytoplasmic domain is as yet undetermined, although lengths of 7, 14, and 20 residues have been proposed (Toyofuku et al., 1994; Young et al., 1989; Simmerman et al., 1989).

The C-terminal 22 residues of PLB are markedly hydrophobic and appear to represent a membrane-anchoring domain. Phospholamban adopts a pentameric form in SDS/polyacrylamide gels at ambient temperature; this oligomer dissociates into monomers upon boiling. At present there is no evidence that domain II binds directly to the Ca^{2+}-ATPase. Furthermore, the pentameric structure does not appear to be required for activity; a mutant form of PLB, which is monomeric when coexpressed with the Ca^{2+}-ATPase, is fully functional (Toyofuku et al., 1994). A model for the pentamer structure has recently been proposed by Arkin et al., based on mutagenesis experiments, in which the transmembrane domains adopt a left-handed coiled-coil helical bundle (Arkin et al., 1994). Residues between Ia and II (termed Ib) have previously been assumed to adopt a random coil or extended conformation, based on the helical content derived from the CD spectrum of the intact native protein (Simmerman, 1989; Vorherr et al., 1993).

Despite a number of studies of the bulk spectroscopic and physicochemical properties of phospholamban, no detailed structural data are available on its solution conformation. In this study, we have employed various spectroscopic methods to determine the conformations of peptides derived from the proposed cytoplasmic domain of phospholamban. Furthermore, we examined the effect of phosphorylation at S16 on the conformation of the same peptide to probe the conformational requirements for regulation of the Ca^{2+}-ATPase by phospholamban.

MATERIALS AND METHODS

Synthesis of PLB Peptides. Chemical synthesis of the PLB(1−25) peptide was performed by solid-phase methodology (Merrifield, 1963), using a double-coupling protocol for the introduction of all amino acids on a Model 430A Applied Biosystems automated peptide synthesizer. Deprotection and removal of the peptide from the resin support were achieved by treatment with liquid hydrofluoric acid (Sakakibara et al., 1967). The peptides were purified by preparative high-performance liquid chromatography on a Vydac reverse-phase C_{18} column (Rivier et al., 1984). The column was equilibrated with 95% buffer A (0.1% trifluoroacetic acid in water) and 5% buffer B (0.1% trifluoroacetic acid in acetonitrile). After injection of the sample a linear gradient was run from 95% buffer A to 50% buffer A over 60 min. Homogeneity of the peptides was demonstrated by analytical HPLC, and identity was confirmed by amino acid composition analysis and mass spectrometry. The phosphorylated PLB(1−25) peptide was obtained by incubating 5 mg of PLB(1−25) with 4000 units of the protein kinase A catalytic subunit (Sigma Chemical Co.) in a reaction buffer containing 10 mM MOPS, 0.1% Zwittergent 3−14, 5 mM $MgCl_2$, and 100 μM ATP for 10 min at 30 °C. The reaction was terminated by addition of an equal volume of 2% SDS. The peptides were then repurified as previously described. Two forms of the PLB(1−25) peptide were used. NMR experiments on PLB(1−25) in 30% TFE were carried out on a R25C mutant. This mutation was introduced to allow the attachment of auxiliary lipids at the C-terminus (C. J. Burke, C. R. Middaugh, V. M. Garsky, and R. G. Johnson, unpublished data), and is not expected to affect significantly the conformation of PLB(1−25). Disulfide formation was inhibited by the addition of small amounts of perdeuterated dithiothreitol; no dimeric species were detected by mass spectrometry. All other experiments were performed on PLB(1−25; R25).

Mass Spectrometry. Mass analysis was performed with a Kratos Analytical MALDI III laser desorption time-of-flight mass spectrometer. Peptide solutions at concentrations of ca. 5 μM were applied to a sample slide (0.3 μL) with 1 μL of 50 mM α-cyano-4-hydroxycinnamic acid (Aldrich). Bovine insulin (Sigma, 0.4 μL, 10 μM) was added to the sample slide as an internal mass calibrant. The sample was allowed to dry before introduction into the instrument. Spectra were acquired in the high-resolution reflectron mode.

Circular Dichroism Spectroscopy. CD spectra were collected on a Jasco J-720 spectropolarimeter calibrated with camphorsulfonic acid. Spectra were recorded using a 1-mm path-length quartz cuvette thermostated at 10 °C. A 10 nm/

min scan rate was employed, and an average of two scans was obtained. CD spectra are expressed as the molar circular dichroism ($\Delta\epsilon$). Solutions contained 10 mM sodium phosphate at pH 7 and a peptide concentration of approximately 60 μM.

Nuclear Magnetic Resonance Spectroscopy. NMR samples were prepared at concentrations varying between 1.8 and 4.0 mM in 90% H_2O/D_2O, 30% TFE-d_3/H_2O or 90% H_2O/300 mM SDS-d_{25} (MSD Isotopes). The pH of all samples was adjusted to 3.0 (uncorrected for deuterium isotope effects) using microliter amounts of NaOH/HCl. CD spectra obtained at pH 3.0 were identical to those acquired at pH 7.0; thus the solution conformation is independent of pH over this range. Spectra were acquired on Bruker AMX-500 and Varian Unity 500 spectrometers operating at 500.13 and 499.87 MHz, respectively, and were referenced to internal sodium (trimethylsilyl)propionate at 0.0 ppm. The following spectra were acquired in all three solvent systems: DQF-COSY (Jeener et al., 1979), TOCSY (100 ms and 300 mixing times; Rance, 1987), and NOESY (100, 200, and 300 ms mixing times; Rance et al., 1983). Two-dimensional spectra were acquired in the phase-sensitive mode with quadrature detection in ω_1 using time-proportional phase incrementation on the AMX-500 (Bodenhausen et al., 1980; Marion & Wüthrich, 1983) and States−Haberkorn−Reuben incrementation on the Unity 500 (States et al., 1982). Solvent signals were suppressed with selective presaturation. Data were processed with a Silicon Graphics Indigo R4000 computer using Felix software (Biosym Technologies) and analyzed using NMRVIEW (Johnson & Blevins, 1994). Data sets were generally multiplied by squared sine-bell window functions and zero filled once in both dimensions before Fourier transformation. Final data set sizes were generally 4096 by 1024 real data points.

Coupling Constant Determination. $^3J_{HN\alpha}$ couplings were determined by convolution of selected COSY and NOESY traces with in-phase and anti-phase stick doublets (Titman & Keeler, 1990).

Structure Calculations. Structure calculations were performed with the distance geometry program DIANA (Güntert et al., 1991a,b) using a REDAC strategy (Güntert & Wüthrich, 1991). NOE distance upper bounds were determined from cross-peak intensities by calibration against known interproton distances in elements of regular secondary structure and by reference to protons of fixed separation (geminal protons and aromatic protons of Y-6). Upper bounds were assigned as 2.5, 3.0, 3.7, and 4.5 Å for backbone−backbone NOEs and 3.0, 3.5, 4.2, and 5.0 Å for all other constraints from homonuclear NOESY spectra. Van der Waals lower bounds were used. Dihedral angle constraints were classified as $-90 < \phi < -40$ for $^3J_{HN\alpha} \leq 5.5$ Hz, $-160 < \phi < -80$ for 8.5 Hz $< {}^3J_{HN\alpha} \leq 10.0$ Hz, and $-140 < \phi < -100$ for $^3J_{HN\alpha} \geq 10.0$ Hz (Pardi et al., 1984).

RESULTS AND DISCUSSION

Characterization of PLB(1−25) and pPLB(1−25) in Aqueous Solution. In 10 mM sodium phosphate buffer at pH 7, the CD spectra of PLB(1−25) and its phosphorylated form are similar and are characterized by a negative peak at 200 nm (Figure 2). Although small differences exist, the spectra suggest that both peptides are primarily unstructured in aqueous solution. Weak negative ellipticity in the 210−230-nm region, however, may indicate that a small amount of transient structure is present. These observations are similar to those of Terzi et al. (1992), who examined a phospholamban construct comprising residues 2−33 and the phosphorylated form of the same peptide.

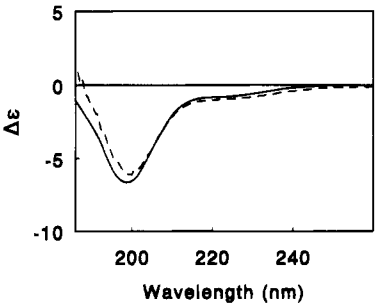

FIGURE 2: Circular dichroism spectra of PLB(1−25) (solid line) and pPLB(1−25) (dashed line) in 10 mM sodium phosphate buffer, pH 7.0.

Other workers have previously obtained ^{1}H assignments for PLB(1−25) in aqueous solution (Gao et al., 1992). No nonsequential NOE connectivities were observed, $d_{NN}(i, i + 1)$ connectivities were absent, and it was concluded that the peptide did not adopt a significantly helical conformation in free solution. We obtained full assignments for both PLB(1−25) and pPLB(1−25) in 90% H_2O/D_2O to explore the effect of phosphorylation on chemical shifts by through-bond and through-space effects. Using a conventional sequential assignment strategy (Billeter et al., 1982), backbone assignments were made for all residues except M1, R13 ($C^\alpha H$), R14, Q23, and C25. Assignments for pPLB(1−25) were made in the same way, although backbone resonances for residues after I18 are severely overlapped and could not be assigned. Phosphorylation results in a downfield shift of S16 NH by 0.25 ppm and downfield shifts of S16 $C^\beta H$ by 0.34 and 0.24 ppm, respectively. No long-range effects on the $C^\alpha H$ shifts of neighboring residues are detected; the $C^\alpha H$ shifts of I12, A15, T17, and I18 are all within 0.03 ppm of their values in the unphosphorylated peptide. A comparison of the published $C^\alpha H$ assignments for both PLB(1−25) and pPLB(1−25) with typical random coil values (Bundi & Wüthrich, 1979) is shown in Figure 3. While there is no NOE evidence for the presence of defined secondary structure, the consistent slight upfield trend present in PLB(1−25) suggests at least helical tendency throughout the peptide (Wright et al., 1988).

Characterization of PLB(1−25) and pPLB(1−25) in 30% Trifluoroethanol/Water. Trifluoroethanol is commonly used to stabilize peptide structure in aqueous solution and has been shown to stabilize helices in peptide fragments from helical regions of proteins (Segawa et al., 1991; Dyson et al., 1992; Sonnichsen et al., 1992). In 30% TFE/H_2O, the CD spectrum of PLB(1−25) has a strong positive signal at 190 nm and negative ellipticity at 207 and 220 nm, features characteristic of helix formation (Figure 4). The spectrum of pPLB(1−25) has peaks of decreasing intensity with a negative peak at 205 nm and a shoulder at 220 nm. Analysis of these spectra by the self-consistent method (Sreerama & Woody, 1993) indicates 60% helical formation by PLB(1−25) decreasing to 27% in the phosphorylated form. The accuracy of these numbers must be tempered by the fact that they are calculated using a globular protein derived database. These data are again in agreement with published data for related,

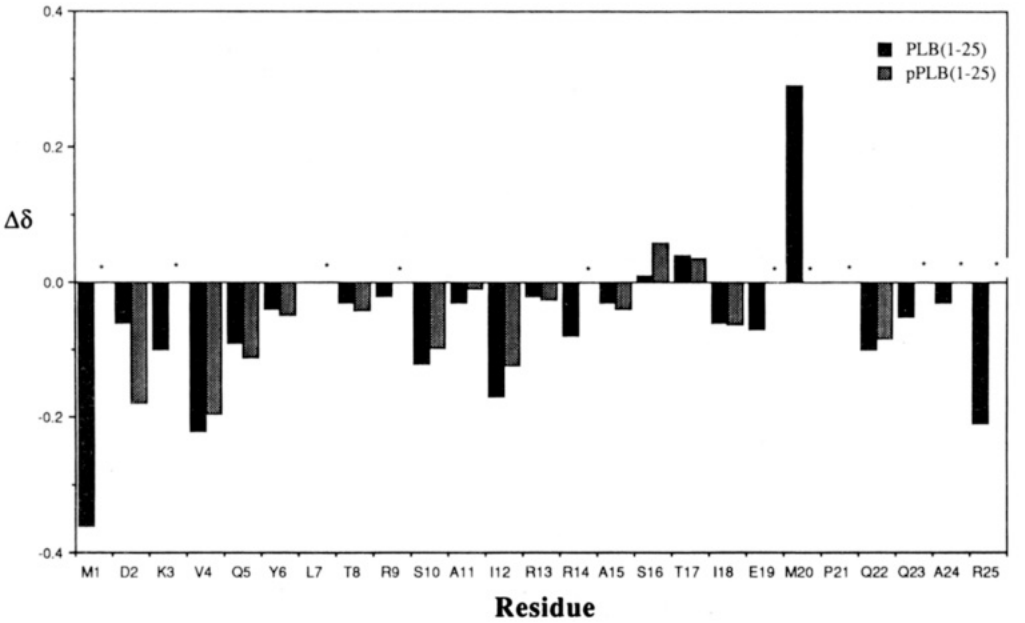

FIGURE 3: Comparison of backbone $C^{\alpha}H$ chemical shifts with random coil values (vertical axis) and residue (horizontal axis) for PLB(1−25) and pPLB(1−25) in 90% H_2O/D_2O, pH 3.0. Resonance assignments for PLB(1−25) are taken from Gao et al. (1992). Starred bars denote residues which could not be assigned due to resonance overlap.

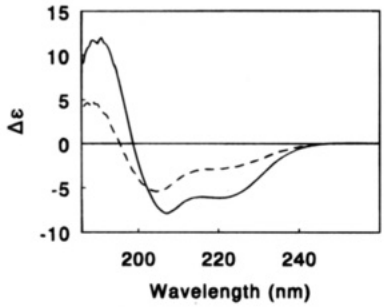

FIGURE 4: Circular dichroism spectra of PLB(1−25) (solid line) and pPLB(1−25) (dashed line) in 30% TFE/10 mM sodium phosphate buffer, pH 7.0.

but longer constructs of the phospholamban cytoplasmic domain. CD measurements provide an estimate of the degree of α-helix formation, but it is not possible to determine the precise location of the helical regions within the sequence. Thus, we examined the solution conformation of PLB(1−25) and pPLB(1−25) in 30% aqueous TFE by NMR.

The fingerprint regions of DQF-COSY experiments acquired for PLB(1−25) in 90% H_2O/D_2O and 30% trifluoroethanol/water, respectively, are shown in Figure 5A,B. The limited NH and $C^{\alpha}H$ shift dispersion observed for PLB(1−25) in water is markedly increased in 30% TFE, consistent with a substantial conformational change or induction of secondary structure. Full assignments for PLB(1−25) in 30% TFE were made from a combination of DQF-COSY, TOCSY, and NOESY experiments using a conventional assignment strategy (Billeter et al., 1982) and are listed in Table 1.

A preliminary identification of secondary structure can be made by inspection of sequential and medium-range NOE connectivities. Thus, helical structure is suggested by a sequence of seven consecutive $d_{NN}(i, i+1)$ NOEs present from M1 to T8 (Figure 6A). T8 and S9 are coincident in chemical shift, precluding the observation of the $d_{NN}(8, 9)$ NOE. Amide chemical shift degeneracy also precludes the unambiguous assignment of NOEs between the NH protons of S10 to R13, but a sequence of three more strong $d_{NN}(i, i+1)$ NOEs can be confidently assigned from R14 to T17. Chemical shift degeneracy of $C^{\alpha}H$ protons is relatively extensive, but a number of medium-range $d_{\alpha N}(i, i+2,3,4)$ NOEs were unambiguously assigned (Figure 6B). These connectivities are consistent with helical secondary structure in the N-terminal 16−17 residues of PLB(1−25). A number of predicted medium-range NOEs of the same type could not be distinguished due to overlap with strong intraresidue and sequential NOEs (dashed lines, Figure 7). No long-range, i.e., greater than $(i, i+4)$ connectivities could be distinguished from any amide signals or from the side-chain aromatic resonances of Y6. This observation is not unusual in a linear helical peptide. Taken together, the observed NOE connectivities are all consistent with helical secondary structure extending from the N-terminal M1 as far as T17. It is notable that evidence for helical secondary structure in residues 18−25 is absent. NOEs such as T17-$C^{\alpha}H$ to M20-NH, P21-$C^{\alpha}H$ to A24-NH, and Q22-$C^{\alpha}H$ to C25-NH all lie in nonoverlapped regions of the spectrum and are not present at baseline levels.

Additional information on polypeptide secondary structure is provided by backbone coupling constants. In general, small $^3J_{HN\alpha}$ couplings (<5.5 Hz) are associated with helical regions of peptides and proteins, while values >8 Hz are expected for extended conformations (Wüthrich, 1986). Spin−spin coupling constants were measured at 300 K for 20 of 24 possible residues by convolution of anti-phase and in-phase traces from DQF-COSY and TOCSY experiments (Titman & Keeler, 1993) (Table 2). Coupling constants for eight residues could also be measured directly from a 1D spectrum acquired under the same conditions and agree with those determined by convolution within the limits of experimental error. Coupling constants for four residues could not be measured directly from the 1D spectrum and had fingerprint cross-peaks which were too severely overlapped to allow the extraction of useful traces for convolution. With the exception of D2 (6.4 Hz), A11 (undetermined), and A15 (undetermined), $^3J_{HN\alpha}$ coupling constants

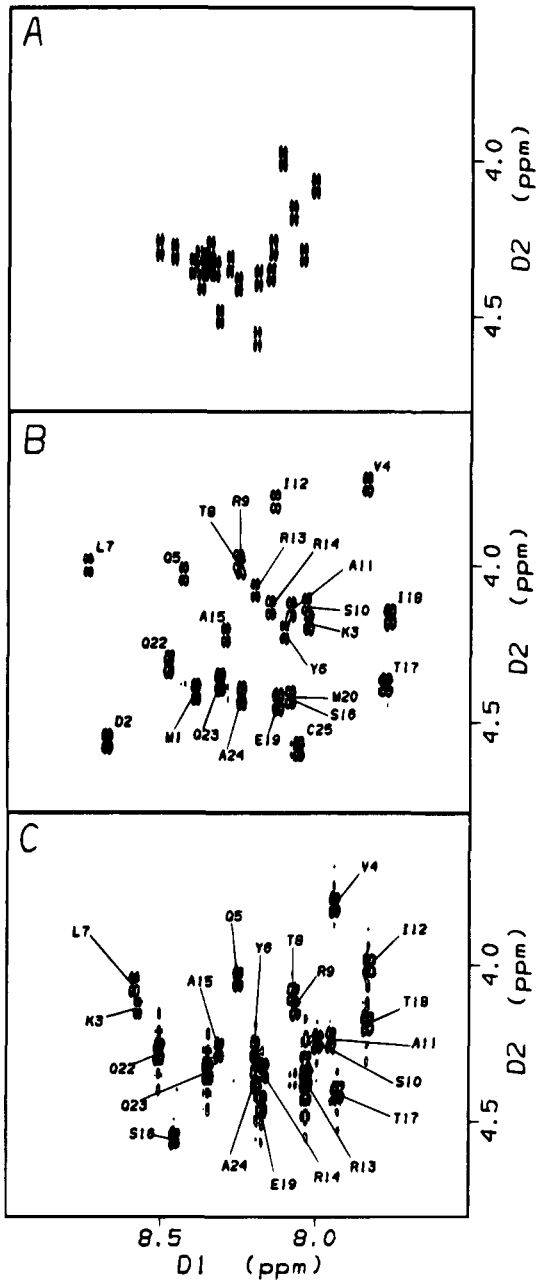

FIGURE 5: Fingerprint regions from DQF-COSY experiments acquired on PLB(1−25) in (A) 90% H_2O/D_2O and (B) 30% TFE, pH 3.05, and on pPLB(1−25) in (C) 30% TFE, pH 3.05. Spectra were recorded at 500 MHz using a 1.8 mM sample of PLB-(1−25).

are uniformly below 5.5 Hz for residues 1−14. S16 appears disordered (7.4 Hz) while the coupling constant determined for T17 (10.6 Hz) suggests an extended conformation at this position.

Solution Structure of PLB(1−25) in 30% TFE. A total of 54 nonredundant distance constraints were identified in the 100 ms NOESY experiment and used with 17 backbone torsion angle constraints as input to the distance geometry program DIANA (Güntert et al., 1991a,b; Güntert & Wüthrich, 1991). The family of conformers is best described by a regular α-helix from residues 1 to 15 (Figure 8). All hydrogen bonds observed to form in more than 10 of 20 conformers were of the *i*, *i*+4 type, consistent with α rather than 3_{10}-helix. The mean rms deviation from the mean structure is 0.79 Å for residues 1−17 inclusive and 2.04 Å

Table 1: ^{1}H Chemical Shift Assignments for PLB(1−25; C25) in 30% TFE in H_2O, pH 3.05, at 300 K

	NH	$C^\alpha H$	$C^\beta H$	$C^\gamma H$	$C^\delta H$	$C^\epsilon H$
M1	8.38	4.41	2.61, 2.65			
D2	8.67	4.57	2.91			
K3	8.02	4.18	1.98	1.48, 1.58	1.75	3.02, $N^\zeta H$ 7.68
V4	7.83	3.74	2.25	0.99, 1.10		
Q5	8.43	4.03	2.15, 2.24	2.39, 2.54		
Y6	8.10	4.22	3.21			
L7	8.73	4.01	1.62, 1.99	1.98	0.96, 0.98	
T8	8.25	3.99	4.30	1.28		
R9	8.24	4.01	1.89	1.66, 1.90	3.16	7.23
S10	8.03	4.13	3.78, 3.95			
A11	8.08	4.15	1.57			
I12	8.13	3.80	1.92	1.16, 1.80, γCH_3 0.86	0.93	
R13	8.19	4.09	1.97	1.67, 1.77	3.20	7.23
R14	8.15	4.14	1.97	1.68, 1.78	3.23	7.22
A15	8.29	4.23	1.54			
S16	8.08	4.42	4.01, 4.07			
T17	7.77	4.39	4.38	1.30		
I18	7.76	4.17	1.97	1.25, 1.59, γCH_3 0.96	0.91	
E19	8.12	4.44	2.03, 2.15	2.50		
M20	8.12	4.41	2.09	2.61, 2.67		
P21		4.46	1.96, 2.36	2.08	3.78, 3.86	
Q22	8.47	4.32	2.04, 2.16	2.44		
Q23	8.31	4.38	2.03, 2.15	2.41		
A24	8.24	4.42	1.46			
C25	8.05	4.59	3.02			

for all heavy atoms in the same region. Residues 18−25 are largely disordered, except that the backbone traces of each conformer subtend away from the axis of the helix over a relatively limited range (approximately 180°). The helix is capped at its C-terminus by hydrogen bonds between S16-NH and I12-CO (13 structures), T17-HG1 and R13-CO (4 structures), and T17-NH and R14-CO (5 structures).

Conformational $C^\alpha H$ Resonance Shifts in PLB(1−25). A number of studies have demonstrated a strong correlation between $C^\alpha H$ secondary shifts (defined as the difference between observed $C^\alpha H$ and "random coil" shifts) and secondary structure in proteins (Szilagyi & Jardetsky, 1989; Williamson, 1990; Wishart et al., 1991). Helical secondary structure is suggested by consistent multiple upfield secondary shifts, while extended β-structure correlates with consistent downfield shifts. This observation is particularly useful in application to peptides with substantial chemical shift degeneracy such as PLB(1−25), since a large number of helix-defining NOEs cannot be reliably assigned but full backbone assignments are available. A plot of secondary chemical shift vs residue number for PLB(1−25) shows a consistent upfield trend for the sequence M1−S16 (Figure 9), with more pronounced upfield shifts for the central residues of this sequence (V4−R13). Wishart and coworkers have quantitated the significance of secondary shift magnitudes by comparison of observed $\Delta\delta$ ($C^\alpha H$) values with average values obtained from residues in known secondary structure in proteins (Wishart et al., 1992). Generally, a >0.1 ppm upfield shift from random coil is associated with α-helical secondary structure, while a similar magnitude downfield shift correlates with β-sheet conformation in proteins. In 90% H_2O/D_2O, PLB(1−25) contains no apparent secondary structure (defined as four or more consecutive +1 or −1 scores).

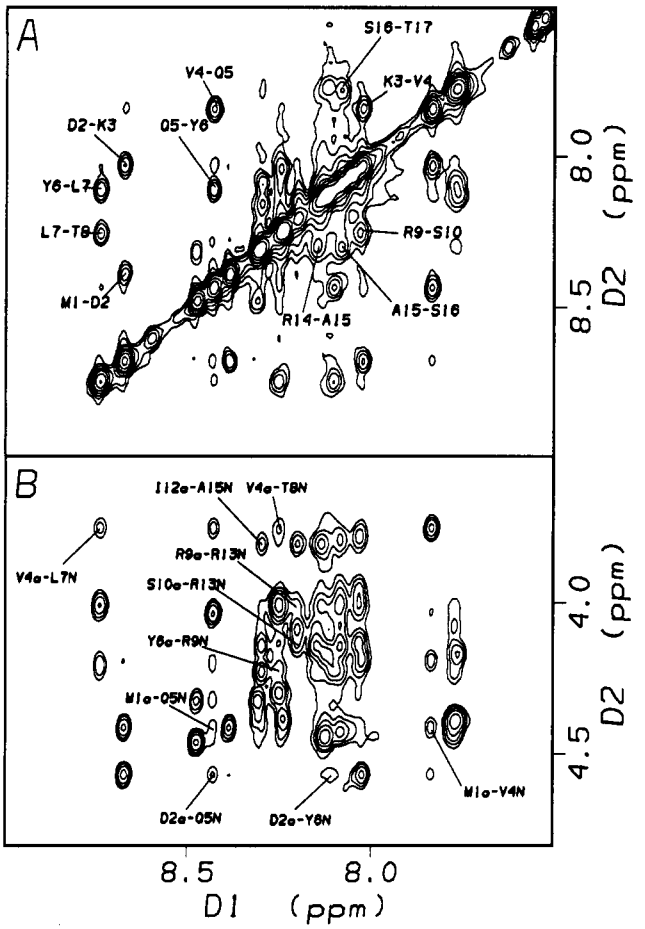

FIGURE 6: Portions of NOESY contour plots for PLB(1−25) in 30% TFE, pH 3.05, at 300 K, acquired with a mixing time of 300 ms: (A) NH−NH region, showing assigned $d_{NN}(i, i+1)$ NOEs; (B) fingerprint region of the same experiment. Medium-range $C^{\alpha}H$−NH (i, $i+2$, 3, and 4) NOEs are labeled.

The observed large $^3J_{HN\alpha}$ coupling constants for T17 and I18 presumably derive from the propensity toward extended structure in consecutive β-branched amino acids. Direct characterization of local structure employing NOEs in this region, however, is hampered by the chemical shift degeneracy of T17/I18 and E19/M20/other amides.

Effect of Phosphorylation upon Secondary Structure. The phosphorylated form of PLB(1−25) was prepared by enzymatic phosphorylation and purified to homogeneity using reverse-phase HPLC. The presence of the completely monophosphorylated form was confirmed by mass spectrometry. The one-dimensional NMR spectrum of pPLB-(1−25) in 30% TFE/water is not markedly different from that of PLB(1−25), except that the amide envelope is somewhat altered. Full assignments were obtained in the same manner as PLB(1−25). The overall pattern of backbone shifts is conserved, with V4 and I12 dispersed from the bulk of fingerprint cross-peaks (Figure 5C). The reduced chemical shift range over which both amide and $C^{\alpha}H$ resonances are distributed in the phosphorylated peptide causes a larger number of structure-defining NOEs to be overlapped compared with PLB(1−25). This is particularly so for residues near the phosphorylation site, and it is not possible unambiguously to distinguish secondary structure in this region purely from NOE data. Nevertheless, useful information about the effect of phosphorylation on structure was obtained from coupling constant and secondary shift data. It is clear that, in aqueous solution, phosphorylation has a localized effect on chemical shifts compared to the unphosphorylated form, influencing only the $C^{\beta}H$ protons of S16. This is consistent with other published data on phosphorylated model peptides (Hoffman et al., 1994). However, in 30% TFE, $\Delta\delta(C^{\alpha}H)$ values for residues 1−15 are substantially different from those of the unphosphorylated peptide. The magnitude of $\Delta\delta(C^{\alpha}H)$ values for this region is decreased by approximately 20% relative to those of PLB-(1−25) (Figure 9A), suggesting an overall decrease in helicity. Furthermore, in residues 13−17, $\Delta\delta(C^{\alpha}H)$ values decrease to approximately zero. The significance of calculated $\Delta\delta(C^{\alpha}H)$ values was quantitated as described previously (Wishart et al., 1992) (Figure 9B). Using these criteria, pPLB(1−25) appears to undergo a local unwinding (or a significant disruption) of the helix after residue 12 when compared to the data for PLB(1−25). A single medium-range NOE can be confidently assigned for peptide residues 12−17, namely, I12-$C^{\alpha}H$ to A15-NH, resolved by virtue of the maintained upfield shift of Ile-12-$C^{\alpha}H$. That this NOE is still present even at mixing times as short as 100 ms, albeit at reduced intensity compared with that in the unphosphorylated form, implies that some type of defined conformation does exist for residues 13−17. A disruption of the helix by five residues corresponds to a decrease in helical secondary structure content from 60% to 40%, in reasonable agreement with α-helical content obtained from the CD spectral analyses of PLB(1−25) and pPLB(1-25) under the same solvent conditions.

While NOE data involving residues near to the phosphorylation site are either ambiguous or unavailable, it was possible to determine $^3J_{HN\alpha}$ coupling constants for a number of resolved cross-peaks by convolution as described previously. Values for S10 and A11 could not be determined, but significant increases in coupling constants were determined for I12 and R13 (Table 2). The coupling constant determined for A15 is also in the disordered range (7.7 Hz), although the value for this residue in PLB(1−25) was indeterminate. $^3J_{HN\alpha}$ couplings for T17 and I18 remain large (10.3 and 9.2 Hz, respectively). These data reinforce the view that phosphorylation disrupts secondary structure in the middle of the phospholamban cytoplasmic domain.

Conformational Studies in Sodium Dodecyl Sulfate Micelles. In the studies described above, trifluoroethanol was used as an inducer of secondary structure in model peptides representing the "cytoplasmic" (i.e., nontransmembrane spanning) domain of phospholamban. However, the isotropic surroundings provided by this solvent system necessarily is not a persuasive model for a natural membrane. An improved model of a membrane environment is provided by micellar solutions of perdeuterated detergents. A large number of membrane-active peptides and small proteins have now been examined in SDS or DPC using both homonuclear and heteronuclear techniques (Macquaire et al., 1992; Rizo et al., 1993; Kohda & Inagaki, 1992; McDonnell & Opella, 1993; Papavoine et al., 1994). We applied this approach to domain Ia of phospholamban to examine the solution conformation of both PLB(1−25) and pPLB(1−25) in perdeuterated SDS micelles.

CD spectra of PLB(1−25) in 2% SDS contain features similar to those exhibited by the peptide in 30% TFE but of lower magnitude (Figure 10). Analysis of the CD spectrum

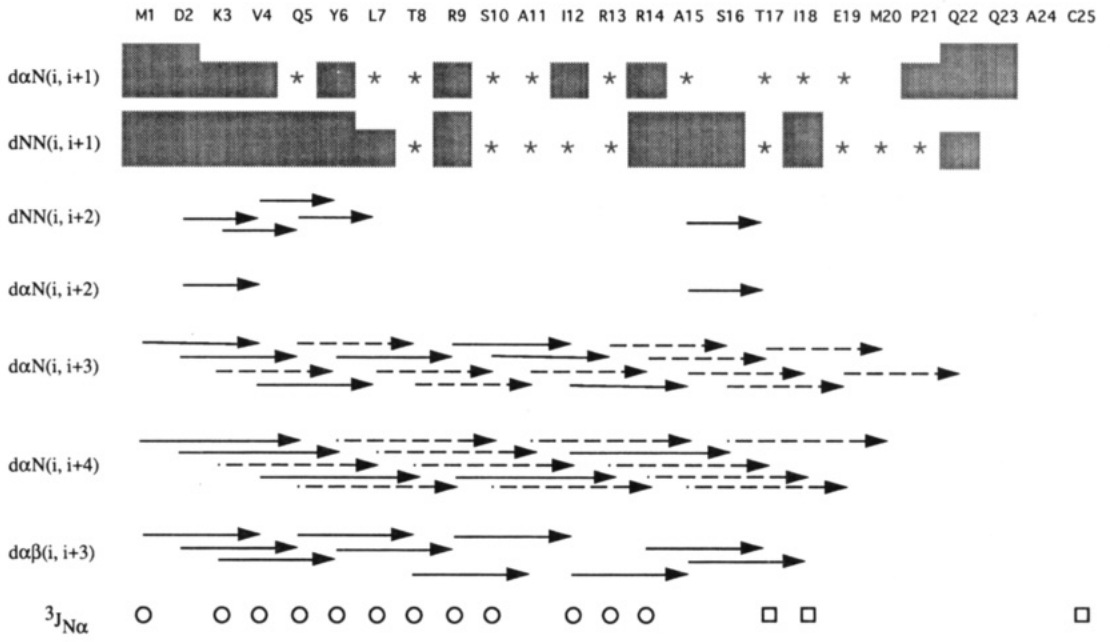

FIGURE 7: Summary of observed sequential and medium-range NOE connectivities for PLB(1−25) in 30% TFE/H_2O, pH 3.05, at 300 K. Assignments were made from NOESY spectra acquired using 100, 200, and 300 ms mixing times. Sequential NOEs are represented by shaded blocks; the height of the block is a qualitative measure of relative NOE intensity. Medium-range NOEs are represented by bars connecting the appropriate residues. NOEs which could not be confidently assigned due to resonance degeneracy but which would be expected in a region of regular helical secondary structure are denoted by dashed lines. Open circles denote $^3J_{N\alpha}$ coupling constants smaller than 5.5 Hz, while open boxes denote values greater than 8.0 Hz.

Table 2: Measured Coupling Constants ($^3J_{HN\alpha}$) for PLB(1−25) and pPLB(1−25) in 30% TFE Obtained by Convolution of COSY and TOCSY Traces with Stick Doublets or by Direct Measurement from One-Dimensional Spectra

	PLB(1−25)		pPLB(1−25)	
residue	convolution	1D	convolution	1D
M1	4.7	4.8		
D2	6.4	5.8	6.7	5.7
K3	4.9	5.3	5.2	
V4	5.1	5.1	5.7	
Q5	3.5	3.8	4.2	
Y6	4.2			
L7	3.9		3.9	4.7
T8	5.4		6.6	
R9	4.5		4.6	
S10	4.8			
A11				
I12	4.8		7.3	
R13	4.1		7.2	
R14	5.3			
A15			7.7	
S16	7.4		7.7	6.8
T17	10.6		10.3	
I18	8.3		9.2	
E19			8.7	
M20	8.0			
P21				
Q22	7.4	6.4	7.0	6.3
Q23	7.9	6.9		
A24				
C25	9.8	7.7		

of PLB(1−25) in SDS finds approximately 40% α-helix. Phosphorylation again results in a substantial decrease in spectral intensity, suggesting about 20% helical content (Figure 10).

^{1}H chemical shift assignments were obtained for PLB(1−25) in 300 mM aqueous SDS-d_{25}, again using a conventional backbone-directed assignment strategy with data from NOESY, TOCSY, and DQF-COSY experiments. Chemical shift degeneracy is substantially increased compared with that in TFE/water; nonetheless, complete backbone and >90% of side-chain assignments could be made. The general pattern of NH−C$^\alpha$H cross-peaks is closely related to that observed in 30% TFE; notably I12 and V4 C$^\alpha$H are upfield shifted. Similarly, T17- and I18-NH remain the most upfield amide resonances (Figure 11). Sequential $d_{\alpha N}(i, i+1)$ NOEs are uniformly low in intensity for residues 1−17 while $d_{NN}(i, i+1)$ NOEs are relatively intense. Medium-range NOEs are detected between V4-C$^\alpha$H and L7-NH and between I12-C$^\alpha$H and A15-NH, although other diagnostic medium-range NOEs are obscured by overlap. Secondary shifts and secondary structure scores were calculated as described previously and are shown in Figure 11. Helical secondary structure is less clearly delineated than in 30% TFE; while residues 3−16 are upfield shifted, I18, M20, Q22, and R25 are also. Nonetheless, using the criterion of Wishart et al. that multiple consecutive upfield shifts are required to define a helical element, our results are consistent with helix formation by approximately the same region in PLB(1−25) in 30% TFE.

DQF-COSY experiments on other similarly sized peptides in detergent micelles frequently fail to exhibit useful fingerprint information (R. J. Mortishire-Smith, unpublished results), presumably due to line-width effects. This is not the case for PLB(1−25) or pPLB(1−25); the fingerprint region of a DQF-COSY experiment obtained with PLB(1−25)/300 mM SDS-d_{25} is shown in Figure 12 (for comparison with 30% TFE, see Figure 5B). Significant differences are observed between the COSY cross-peak intensities for residues 1−17 (which have weak intensities) compared with residues 18 and beyond. These differences are not apparent in spectra acquired in aqueous TFE. The most likely explanation for these differences is that the residues involved in helix formation are directly associated with the detergent micelle and therefore have a correlation time close to that of the (much larger) micelle and a correspondingly large line

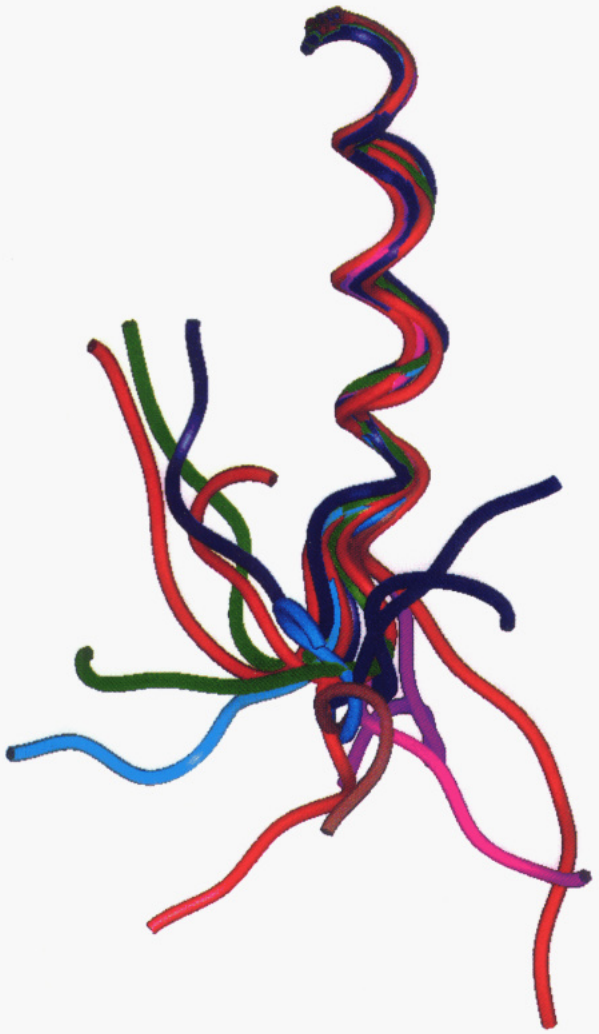

FIGURE 8: Overlay of 20 calculated conformers of PLB(1−25) on residues 1−16.

width. Given the reduced $^3J_{HN\alpha}$ coupling constant for helical residues, the intensities of cross-peaks from residues 1−17 will be reduced (Neuhaus et al., 1985). By contrast, the disordered residues 18−25 are probably not directly micelle-associated but are relatively freely rotating. $^3J_{HN\alpha}$ couplings for random coil conformations are inherently larger than those for helices; together these effects result in substantially increased cross-peak intensities.

The NMR spectrum of phosphorylated peptide pPLB(1−25) was also assigned in detergent micelles, and secondary structure was evaluated on the basis of sequential/medium-range NOE connectivities and secondary shifts. In contrast to the same peptide in TFE/water, in which the $C^{\alpha}H$ $\Delta\delta$ values for residues 12−16 are uniformly reduced to near zero, in SDS-d_{25} significant effects are limited to R13 and S16 (Figure 11B). The $\Delta\delta$ value for R14 is unchanged; while reduced in magnitude, A15 retains a helical score. This is consistent with a model in which phosphorylation induces a perturbation in secondary structure with effects, perhaps localized, to one face of the helix. A possible source of this perturbation might be the generation of a salt bridge between the protonated guanidinium side chain of R13 and the negatively charged phosphate group of S16 in pPLB(1−25).

Secondary Structure Quantitation by NMR. Elements of secondary structure in medium-sized peptides are unlikely to be fixed entities in solution. For instance, local breathing

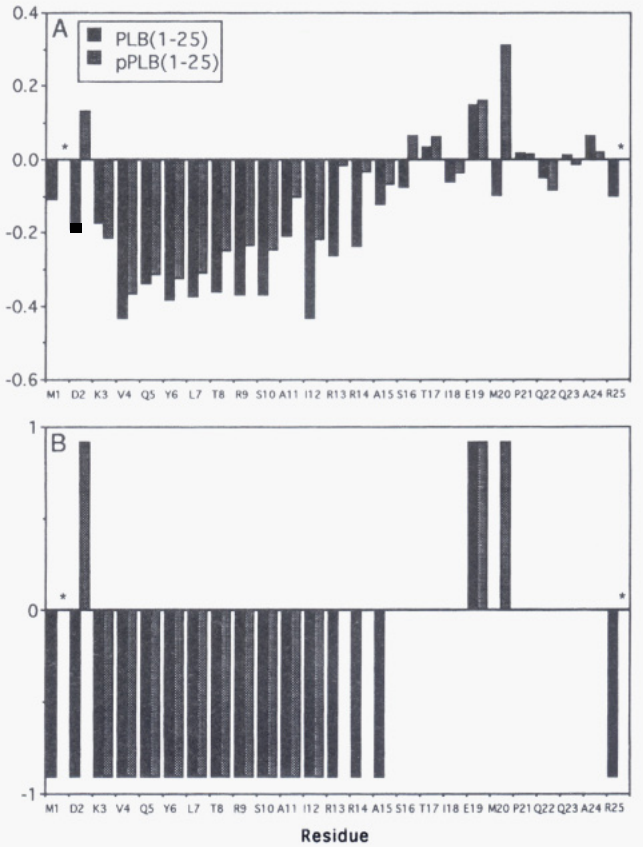

FIGURE 9: (A) Secondary shifts ($\Delta\delta$, vertical axis) for $C^{\alpha}H$ resonances of PLB(1−25) (heavy bars) and pPLB(1−25) (shaded bars) by residue (horizontal axis) in 30% TFE/H_2O, pH 3.05, at 298 K, defined as the difference between the observed chemical shift and the published random coil chemical shift for each residue. Negative (upfield) $\Delta\delta$ values are associated with helical secondary structure and positive (downfield) $\Delta\delta$ values with β structure. (B) Secondary structure scores (residues deemed significantly shifted from random coil values) determined according to the method of Wishart et al. (see text). Starred bars denote $C^{\alpha}H$ shifts not measurable.

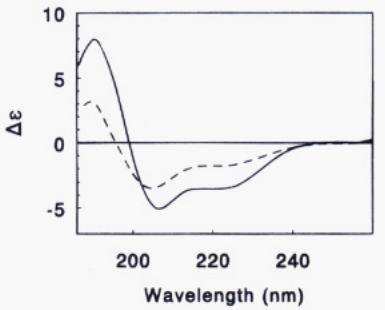

FIGURE 10: Circular dichroism spectra of PLB(1−25) (solid line) and pPLB(1−25) (dashed line) in 2% SDS/10 mM phosphate buffer, pH 7.0.

within helices is observed in amide exchange experiments where exchange half-lives typically are on the order of hours. The measured secondary structure content of a peptide is thus a combination of the extent to which secondary structure is formed, together with its lifetime over the observable time scale. Direct estimation of secondary structure is possible from CD and FTIR spectra, although the degree of structure may be underestimated due to the longer observation time scale. It is also possible semiquantitatively to determine secondary structure content by averaging conformationally dependent $C^{\alpha}H$ shifts, using the assumption that $C^{\alpha}H$ protons undergoing fast interconversion between helical and disor-

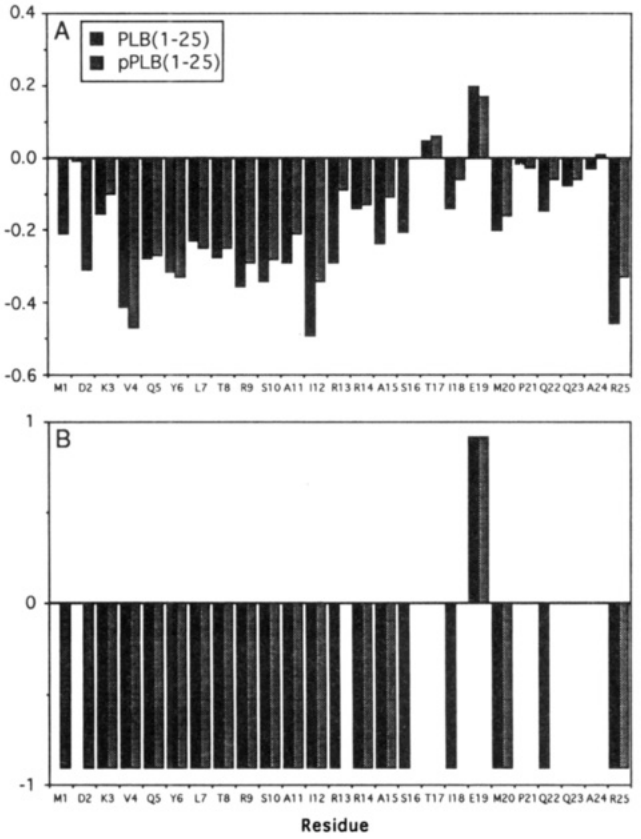

FIGURE 11: (A) $\Delta\delta$ values for PLB(1−25) in 300 mM SDS-d_{25} at pH 3.10 and 305 K and for pPLB(1−25) in 300 mM SDS-d_{25} at pH 3.14 and 305 K. (B) Secondary structure scores quantitated according to Wishart et al. (see text).

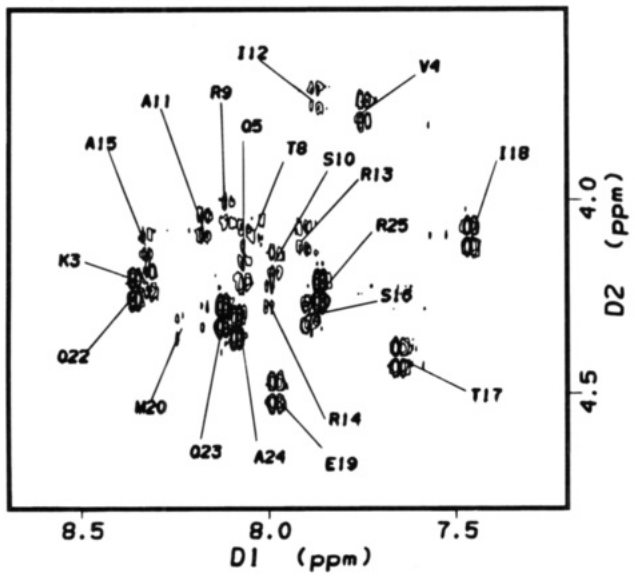

FIGURE 12: Fingerprint region of a DQF-COSY experiment acquired on PLB(1−25) in 300 mM aqueous SDS-d_{25}, pH 3.10, at 305 K.

dered conformations will exhibit upfield secondary shifts proportional to the time spent in each state (Rizo et al., 1993). We estimated the helical content of PLB(1−25) and pPLB-(1−25) in TFE and SDS by summing the observed upfield shifts over residues 1−16 and the full-length peptide and then dividing by the predicted "total" upfield shift for the relevant region, defined as 0.35 ppm multiplied by the appropriate number of residues (Rizo et al., 1993) (Table 3). Thus, assuming that the helix in PLB(1−25) extends

Table 3: Helical Secondary Structure Quantitated by Summing the Secondary Shifts over either Residues 1−16 or Residues 1−25 and Dividing by 0.35 × n Residues[a]

	NMR		CD	
	TFE	SDS	TFE	SDS
PLB(1−25)	1−16, 80%; 1−25, 51%	1−16, 72%; 1−25, 55%	60%	40%
pPLB(1−25)	1−12, 60%; 1−16, 49%; 1−25, 29%	1−16, 65%; 1−25, 46%	27%	20%

[a] 0.35 ppm represents the upfield shift for a residue completely helical 100% of the time. Values for the equivalent CD spectrum determined by structure analysis are also shown

from residues 1 to 16, this helix is populated approximately 80% of the time. As judged by coupling constants and individual secondary shifts, the helix in pPLB(1−25) extends only as far as residue 12. However, the estimated population of helical secondary structure in residues 1−16 of the latter peptide decreases to 60%, indicating once more that phosphorylation has a systemic effect on helical stability as well as more local effects on conformation.

CONCLUSIONS

In this study, we attempted to determine the solution structures of peptides representing domain Ia of phospholamban in apolar environments designed to stabilize native-like structure. Direct characterization of intact phospholamban is hampered in two ways: it exhibits extreme insolubility in conventional aqueous/alcoholic media and has a propensity to form pentamers in detergents. Other workers have previously shown that the nonmembrane-spanning domains of phospholamban (residues 1−32) adopt a predominantly helical conformation in aqueous solutions of detergents and alcohols. Thus, PLB(2−33) adopts approximately 33% helical content in 40% TFE, with phosphorylation at S16 inducing a drop of approximately 8% in helical content (Terzi et al., 1992). By contrast, when studied in a non-structure-inducing solvent (5 mM phosphate buffer), PLB(2−33) is slightly *less* structured than the phosphorylated form (Terzi et al., 1992). This induction of structure may be caused by the formation of R13/R14−S16(PO_3^{2-}) salt bridges in the phosphorylated peptide. Secondary structure prediction algorithms also suggest a preferred helical conformation for domain Ia. Nonetheless, none of these results define the precise position or extent of helix formation in domain I.

In aqueous solution PLB(1−25) does not appear to adopt a defined conformation. CD spectra acquired at increasing concentrations of trifluoroethanol exhibit increased helical content with an estimated α-helical content of PLB(1−25) in 30% TFE of 60%. As shown in this work, the solution conformation of PLB(1−25) in aqueous trifluoroethanol comprises a regular α-helix spanning residues 1−16/17, with the C-terminal 7/8 residues essentially disordered. Some evidence for an extended conformation around residues 20−22 is provided by downfield secondary shifts, but resonance degeneracy in this region hampers direct characterization of structure.

In aqueous trifluoroethanol, the phosphorylated peptide undergoes an unwinding/disruption of structure localized within the C-terminal five residues of the α-helix; a 25%

decrease in the magnitude of $\Delta\delta$ values for residues 1−11 may reflect an associated decrease in the stability of the remainder of the helix. That a medium-range NOE I12-C^{α}H−A15-NH is still observed in pPLB(1−25), albeit substantially attenuated compared with the *apo* form, implies that the C-terminal 1.5 turns of helix are not completely unwound. Certainly though, the structure is sufficiently disordered to remove the source of upfield secondary shifts. Evidence that the $\Delta\delta$ changes are not solely due to a through-space effect from the introduced phosphate group is two-fold. First, when studied in 10 mM phosphate buffer, chemical shift differences between *apo* and *phospho* forms are limited to the C^{β}H protons of S16. Second, CD spectra also clearly indicate a decrease in helical contributions on phosphorylation. Dissociation of the PLB/ATPase complex is presumably also influenced by charge repulsion from the negatively charged phosphate group.

The secondary structure of PLB(1−25) determined in 300 mM SDS-d_{25} is similar to that determined in trifluoroethanol/water. Both upfield secondary shifts and observed $d_{NN}(i, i+1)$ NOEs, together with a smaller number of resolved $d_{\alpha N}(i, i+3)$ NOEs, are consistent with formation of a helix by the first 16/17 residues. However, the disruption of the helix is more localized than in TFE/water and appears limited to one face of the helix. Charge−charge interactions between the R13 guanidinium and S16 phosphate groups appear a likely cause of the observed structural changes. Ultimately, the dynamics of peptides and proteins are best dissected by an analysis of heteronuclear relaxation data, and work is in progress to characterize labeled PLB constructs. These will also facilitate structure determination of the phosphorylated form, since resonance degeneracies within backbone amide signals can be resolved by virtue of dispersion in ^{15}N shifts.

The work described here was carried out in order to better understand interactions within the PLB/ATPase complex. The simplest model for this requires that the dominant interactions involve the C-terminus of the cytoplasmic α-helix, perhaps invoking hydrogen bonds between the ATPase and S16 side chain. Introduction of the double negative charge then disrupts these interactions, and the complex dissociates. Alternatively, it may be that the entire cytoplasmic helix forms a recognition unit, and the altered dynamics of this region of PLB upon phosphorylation induce an instability and consequent lowered affinity for the ATPase. MacLennan and co-workers have previously shown that appropriate mutations in the first 6−8 residues result in PLB variants that are unable to bind the ATPase, suggesting that this region of the cytoplasmic domain contributes to the binding energy of the complex (Toyofuku et al., 1994). The same arguments apply, however, to these mutations, which may act either by disrupting a specific required PLB−ATPase interaction or by destabilizing the entire recognition unit. We are presently characterizing a number of PLB mutants to discern which of these mechanisms is appropriate. Although significant data indicate it is the cytoplasmic domain of PLB that directly binds to the Ca^{2+}-ATPase, a contribution of the transmembrane region through a direct interaction with the ATPase or stabilization of the PLB-cytoplasmic domain cannot be excluded (Jones & Field, 1993). Characterization of the full-length PLB will be ultimately required.

ACKNOWLEDGMENT

We are grateful to Drs. D. Neuhaus and S. Opella for helpful discussions and to E. Mayer for peptide phosphorylation.

REFERENCES

Arkin, I. T., Adams, P. D., MacKenzie, K. R., Lemmon, M. A., Brünger, A. T., & Engelman, D. M. (1994) *EMBO J. 13*, 4757−4764.
Billeter, M., Braun, W., & Wüthrich, K. (1982) *J. Mol. Biol. 155*, 321−346.
Bodenhausen, G., Vold, R. I., & Vold, R. R. (1980) *J. Magn. Reson. 55*, 301−315.
Briggs, F. N., Lee, K. F., Wechsler, A. W., & Jones, L. R. (1992) *J. Biol. Chem. 267*, 26056−26061.
Bundi, A., & Wüthrich, K. (1979) *Biopolymers 18*, 285−298.
Byler, D. M., & Susi, H. (1986) *Biopolymers 25*, 469−487.
Dyson, H. J., Merutka, G., Waltho, J. P., Lerner, R. A., & Wright, P. E. (1992) *J. Mol. Biol. 226*, 795−817.
Gao, Y., Levine, B. A., Mornet, D., Slatter, D. A., & Strasberg, G. M. (1992) *Biochim. Biophys. Acta 1160*, 22−34.
Güntert, P., & Wüthrich, K. (1991) *J. Biomol. NMR 1*, 447−456.
Güntert, P., Braun, W., & Wüthrich, K. (1991a) *J. Mol. Biol. 317*, 517−530.
Güntert, P., Qian, Y. Q., Otting, G., Müller, M., Gehring, W., & Wüthrich, K. (1991b) *J. Mol. Biol. 217*, 531−540.
Hicks, M., Shigekawa, M., & Katz, A. M. (1979) *Circ. Res. 44*, 383−391.
Hoffman, R., Reichert, I., Wachs, W. O., Zeppezauer, M., & Kalbitzer, H. R. (1994) *Int. J. Pept. Protein Res. 44*, 193−198.
Hughes, G., East, J. M., & Lee, A. G. (1994) *Biochem. J. 303*, 511−516.
Inui, M., Chamberlain, B. K., Saito, A., & Fleischer, S. (1986) *J. Biol. Chem. 261*, 1794−1800.
James, P., Inui, M., Tada, M., Ciesi, M., & Carafoli, E. (1990) *Nature 342*, 90−92.
Jeener, J., Meier, B. H., Backmann, P., & Ernst, R. R. (1979) *J. Chem. Phys. 71*, 4546−4553.
Johnson, B. A., & Blevins, R. A. (1994) *J. Biomol. NMR 4*, 603−614.
Jones, L. R., & Field, L. J. (1993) *J. Biol. Chem. 268*, 11486−11488.
Kimura, Y., Inui, M., Kadoma, M., Kijima, Y., Sasaki, T., & Tada, M. (1991) *J. Mol. Cell. Cardiol. 23*, 1223−1230.
Kirchberger, M. A., Borchman, D., & Kasinathan, C. (1986) *Biochemistry 25*, 5484-5492.
Kohda, D., & Inagaki, F. (1992) *Biochemistry 31*, 677−685.
Kranias, E. G. (1985) *J. Biol. Chem. 260*, 11006−11010.
Luo, W., Grupp, I. L., Harrer, J., Ponniah, S., Grupp, G., Duffy, J. J., Doetschman, T., & Kranias, E. G. (1994) *Circ. Res. 75*, 401−409.
Macquaire, F., Baleux, F., Giaccobi, E., Huynh-Dinh, T., Neumann, J-M., & Sanson, A. (1992) *Biochemistry 31*, 2576−2582.
Marion, D., & Wüthrich, K. (1983) *Biochem. Biophys. Res. Commun. 113*, 967−974.
McDonnell, P. A., & Opella, S. J. (1993) *J. Magn. Reson. 102(B)*, 120−125.
Merrifield, R. B. (1963) *J. Am. Chem Soc. 85*, 2149−2154.
Movsesian, M. A., Nishikawa, M., & Adelstein, R. S. (1984) *J. Biol. Chem. 259*, 8029−8032.
Neuhaus, D., Wagner, G., Vasák, M., Kägi, J. H. R., & Wüthrich, K. (1985) *Eur. J. Biochem. 151*, 257−273.
Papavoine, C. H. M., Konings, R. N. H., Hilbers, C. W., & van de Ven, F. J. M. (1994) *Biochemistry 33*, 12990−12997.
Pardi, A., Billeter, M., & Wüthrich, K. (1984) *J. Mol. Biol. 180*, 741−751.
Rance, M. (1987) *J. Magn. Reson. 74*, 557−564.
Rance, M., Sorensen, O. W., Bodenhausen, G., Wagner, E. R. R., & Wüthrich, K. (1983) *Biochem. Biophys. Res. Commun. 117*, 479−485.
Rivier, J., McClentock, R., & Anderson, H. (1984) *J. Chromatogr. 288*, 303−328.
Rizo, J., Blanco, F. J., Kobe, B., Bruch, M., & Gierasch, L. M. (1993) *Biochemistry 32*, 4881−4894.

Sakakibara, S., Shimonishi, Y., Kishida, Y., Okada, M., & Sugihara, H. (1967) *Bull. Chem. Soc. Jpn. 40*, 2164−2167.
Segawa, S. I., Fukuno, T., Fujiwara, K., & Noda, Y. (1991) *Biopolymers 31*, 497−509.
Sham, J. S. K., Jones, L. R., & Morad, M. (1991) *Am. J. Physiol. 261*, H1344−H1349.
Simmerman, H. K. B., Lovelace, D. E., & Jones, L. R. (1989) *Biochim. Biophys. Acta 997*, 322−329.
Sönnichsen, F. D., Van Eyk, J. E., Hodges, R. S., & Sykes, B. D. (1992) *Biochemistry 31*, 8790−8798.
Sreerama, N., & Woody, R. W. (1993) *Anal. Biochem. 209*, 32−44.
States, D. J., Haberkorn, R. A., & Reuben, D. J. (1982) *J. Magn. Reson. 48*, 286-292.
Suzuki, T., & Wang, J. H. (1986) *J. Biol. Chem. 261*, 7018−7023.
Szilagyi, L., & Jardetsky, O. (1989) *J. Magn. Reson. 93*, 441−449.
Tada, M., & Katz, A. (1982) *Annu. Rev. Physiol. 44*, 401−423.
Tada, M., & Kadoma, M. (1989) *BioEssays 10*, 157−163.
Tada, M., Kirchberger, M. A., Repke, D. I., & Katz, A. M. (1974) *J. Biol. Chem. 249*, 6174−6180.
Terzi, E., Poteur, L., & Trifilieff, E. (1992) *FEBS Lett. 309* (3), 413−416.
Titman, J. J., & Keeler, J. H. (1990) *J. Magn. Reson. 89*, 640−646.
Toyofuku, T., Kurzydlowski, K., Lytton, J., & MacLennan, D. H. (1992) *J. Biol. Chem. 267*, 14490−14496.
Toyofuku, T., Kurzydlowski, K., Lytton, J., & MacLennan, D. H. (1993) *J. Biol. Chem. 268*, 2809−2815.
Toyofuku, T., Kurzydlowski, K., Lytton, J., & MacLennan, D. H. (1994) *J. Biol. Chem. 269*, 3088−3094.
Vorherr, T., Wrzosek, A., Chiesi, M., & Carafoli, E. (1993) *Protein Sci. 2*, 339−347.
Williamson, M. P. (1990) *Biopolymers 29*, 1423−1431.
Wishart, D. S., Sykes, B. D., & Richards, F. M. (1991) *J. Mol. Biol. 222*, 311−333.
Wishart, D. S., Sykes, B. D., & Richards, F. M. (1992) *Biochemistry 31*, 1647−1651.
Wright, P. E., Dyson, H. J., & Lerner, R. A. (1988) *Biochemistry 27*, 7167−7175.
Wüthrich, K. (1986) *NMR of Proteins and Nucleic Acids*, Wiley, New York.
Young, E. F., McKee, M. J., Ferguson, D. G., & Kranias, E. G. (1989) *Membr. Biochem. 8*, 95−106.

BI9503007